

Generalization to New Actions in Reinforcement Learning

Ayush Jain^{*1} Andrew Szot^{*1} Joseph J. Lim¹

Abstract

A fundamental trait of intelligence is the ability to achieve goals in the face of novel circumstances, such as making decisions from new action choices. However, standard reinforcement learning assumes a fixed set of actions and requires expensive retraining when given a new action set. To make learning agents more adaptable, we introduce the problem of zero-shot generalization to new actions. We propose a two-stage framework where the agent first infers action representations from action information acquired separately from the task. A policy flexible to varying action sets is then trained with generalization objectives. We benchmark generalization on sequential tasks, such as selecting from an unseen tool-set to solve physical reasoning puzzles and stacking towers with novel 3D shapes. Videos and code are available at <https://sites.google.com/view/action-generalization>.

1. Introduction

Imagine making a salad with an unfamiliar set of tools. Since tools are characterized by their behaviors, you would first inspect the tools by interacting with them. For instance, you can observe a blade has a thin edge and infer that it is sharp. Afterward, when you need to cut vegetables for the salad, you decide to use this blade because you know sharp objects are suitable for cutting. Like this, humans can make selections from a novel set of choices by observing the choices, inferring their properties, and finally making decisions to satisfy the requirements of the task.

From a reinforcement learning perspective, this motivates an important question of how agents can adapt to solve tasks with previously unseen actions. Prior work in deep rein-

^{*}Equal contribution ¹Department of Computer Science, University of Southern California, California, USA. Correspondence to: Ayush Jain <ayushj@usc.edu>, Andrew Szot <szot@usc.edu>.

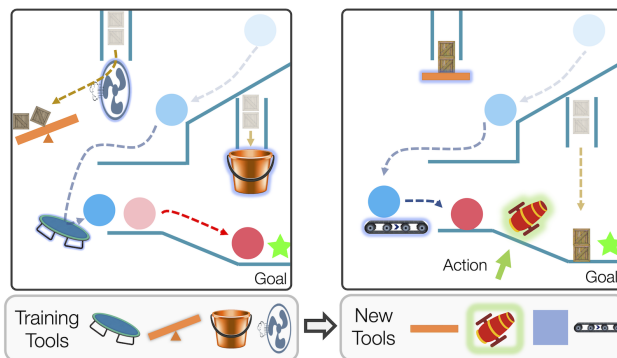


Figure 1. An illustration of zero-shot generalization to new actions in a sequential decision-making task, CREATE. (Left) Learning to select and place the right tools for reaching the goal. (Right) Generalizing the learned policy to a previously unseen set of tools.

forcement learning has explored generalization of policies over environments (Cobbe et al., 2018; Nichol et al., 2018), tasks (Finn et al., 2017; Parisi et al., 2018), and agent morphologies (Wang et al., 2018; Pathak et al., 2019). However, zero-shot generalization of policies to new discrete actions has not yet been explored. The primary goal of this paper is to propose the problem of generalization to new actions. In this setup, a policy that is trained on one set of discrete actions is evaluated on its ability to solve tasks zero-shot with new actions that were unseen during training.

Addressing this problem can enable robots to solve tasks with a previously unseen toolkit, recommender systems to make suggestions from newly added products, and hierarchical reinforcement learning agents to use a newly acquired skill set. In such applications, retraining with new actions would require prohibitively costly environment interactions. Hence, zero-shot generalization to new actions without retraining is crucial to building robust agents. To this end, we propose a framework and benchmark it on using new tools in the CREATE physics environment (Figure 1), stacking of towers with novel 3D shapes, reaching goals with unseen navigation skills, and recommending new articles to users.

We identify three challenges faced when generalizing to new actions. Firstly, an agent must observe or interact with the actions to obtain data about their characteristics. This data can be in the form of videos of a robot interacting with various tools, images of inspecting objects from different

viewpoints, or state trajectories observed when executing skills. In present work, we assume such action observations are given as input since acquiring them is domain-specific. The second key challenge is to extract meaningful properties of the actions from the acquired action observations, which are diverse and high-dimensional. Finally, the task-solving policy architecture must be flexible to incorporate new actions and be trained through a procedure that avoids overfitting (Hawkins, 2004) to training actions.

To address these challenges, we propose a two-stage framework of representing the given actions and using them for a task. First, we employ the hierarchical variational autoencoder (Edwards & Storkey, 2017) to learn action representations by encoding the acquired action observations. In the reinforcement learning stage, our proposed policy architecture computes each given action’s utility using its representation and outputs a distribution. We observe that naive training leads to overfitting to specific actions. Thus, we propose a training procedure that encourages the policy to select diverse actions during training, hence improving its generalization to unseen actions.

Our main contribution is introducing the problem of generalization to new actions. We propose four new environments to benchmark this setting. We show that our proposed two-stage framework can extract meaningful action representations and utilize them to solve tasks by making decisions from new actions. Finally, we examine the robustness of our method and show its benefits over retraining on new actions.

2. Related Work

Generalization in Reinforcement Learning: Our proposed problem of zero-shot generalization to new discrete action-spaces follows prior research in deep reinforcement learning (RL) for building robust agents. Previously, state-space generalization has been used to transfer policies to new environments (Cobbe et al., 2018; Nichol et al., 2018; Packer et al., 2018), agent morphologies (Wang et al., 2018; Sanchez-Gonzalez et al., 2018; Pathak et al., 2019), and visual inputs for manipulation of unseen tools (Fang et al., 2018; Xie et al., 2019). Similarly, policies can solve new tasks by generalizing over input task-specifications, enabling agents to follow new instructions (Oh et al., 2017), demonstrations (Xu et al., 2017), and sequences of sub-tasks (Andreas et al., 2017). Likewise, our work enables policies to adapt to previously unseen action choices.

Unsupervised Representation Learning: Representation learning of high-dimensional data can make it easier to extract useful information for downstream tasks (Bengio et al., 2013). Prior work has explored downstream tasks such as classification and video prediction (Denton & Birodkar, 2017), relational reasoning through visual representation of

objects (Steenbrugge et al., 2018), domain adaptation in RL by representing image states (Higgins et al., 2017b), and goal representation in RL for better exploration (Laversanne-Finot et al., 2018) and sample efficiency (Nair et al., 2018). In this paper, we leverage unsupervised representation learning of action observations to achieve generalization to new actions in the downstream RL task.

Learning Action Representations: In prior work, Chen et al. (2019); Chandak et al. (2019); Kim et al. (2019) learn a latent space of discrete actions during policy training by using forward or inverse models. Tennenholtz & Mannor (2019) use expert demonstration data to extract contextual action representations. However, these approaches require a predetermined and fixed action space. Thus, they cannot be used to infer representations of previously unseen actions. In contrast, we learn action representations by encoding action observations acquired independent of the task, which enables zero-shot generalization to novel actions.

Applications of Action Representations: Continuous representations of discrete actions have been primarily used to ease learning in large discrete action spaces (Dulac-Arnold et al., 2015; Chandak et al., 2019) or exploiting the shared structure among actions for efficient learning and exploration (He et al., 2015; Tennenholtz & Mannor, 2019; Kim et al., 2019). Concurrent work from Chandak et al. (2020) learns to predict in the space of action representations, allowing efficient finetuning when new actions are added. In contrast, we utilize action representations learned separately, to enable zero-shot generalization to new actions in RL.

3. Problem Formulation

In order to build robust decision-making agents, we introduce the problem setting of generalization to new actions. A policy that is trained on one set of actions is evaluated on its ability to utilize unseen actions without additional retraining. Such zero-shot transfer requires additional input that can illustrate the general characteristics of the actions. Our insight is that action choices, such as tools, are characterized by their general behaviors. Therefore, we record a collection of an action’s behavior in diverse settings in a separate environment to serve as action observations. The action information extracted from these observations can then be used by the downstream task policy to make decisions. For instance, videos of an unseen blade interacting with various objects can be used to infer that the blade is sharp. If the downstream task is cutting, an agent can then reason to select this blade due to its sharpness.

3.1. Reinforcement Learning

We consider the problem family of episodic Markov Decision Processes (MDPs) with discrete action spaces. MDPs

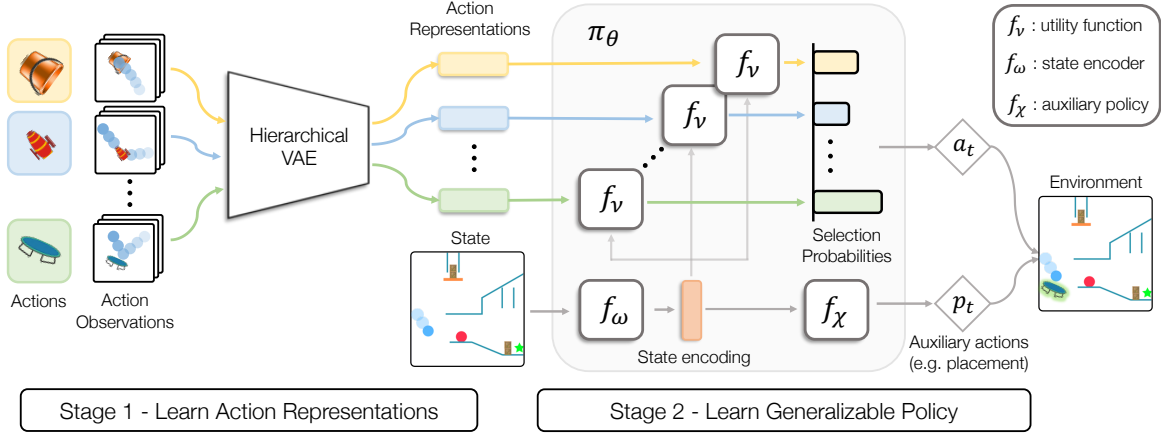


Figure 2. Two-stage framework for generalization to new actions through action representations. (1) For each available action, a hierarchical VAE module encodes the action observations into action representations and is trained with a reconstruction objective. (2) The policy π_θ encodes the state with state encoder $f_\omega(s)$ and pairs it with each action representation using the utility function f_ν . The utility scores are computed for each action and output to a categorical distribution. The auxiliary network takes the encoded state and outputs environment-specific auxiliary actions such as tool placement in CREATE. The policy architecture is trained with policy gradients.

are defined by a tuple $\{\mathcal{S}, \mathcal{A}, \mathcal{T}, \mathcal{R}, \gamma\}$ of states, actions, transition probability, reward function, and discount factor. At each time step t in an episode, the agent receives a state observation $s_t \in \mathcal{S}$ from the environment and responds with an action $a_t \in \mathcal{A}$. This results in a state transition to s_{t+1} and a state-conditioned reward $\mathcal{R}(s_{t+1})$. The objective of the agent is to maximize the expected discounted reward $R = \sum_{t=1}^T \gamma^{t-1} \mathcal{R}(s_t)$ in an episode of length T .

3.2. Generalization to New Actions

The setting of generalization to new actions consists of two phases: training and evaluation. During training, the agent learns to solve tasks with a given set of actions $\mathbb{A} = \{a_1, \dots, a_N\}$. During each evaluation episode, the trained agent is evaluated on a new action set \mathcal{A} sampled from a set of unseen actions \mathbb{A}' . The objective is to learn a policy $\pi(a|s, \mathcal{A})$, which maximizes the expected discounted reward using any given action set $\mathcal{A} \subset \mathbb{A}'$,

$$R = \mathbb{E}_{\mathcal{A} \subset \mathbb{A}', a \sim \pi(a|s, \mathcal{A})} \left[\sum_{t=1}^T \gamma^{t-1} \mathcal{R}(s_t) \right]. \quad (1)$$

For each action $a \in \mathbb{A} \cup \mathbb{A}'$, the set of acquired action observations is denoted with $\mathcal{O} = \{o_1, \dots, o_n\}$. Here, each $o_j \in \mathcal{O}$ is an observation for the action like a state-trajectory, a video, or an image, indicating the action’s behavior. For the set of training actions \mathbb{A} , we denote the set of associated actions observations as $\mathbb{O} = \{\mathcal{O}_1, \dots, \mathcal{O}_N\}$.

4. Approach

Our approach for generalization to new actions is based on the intuition that humans make decisions from new options by exploiting prior knowledge about the options (Gersh-

man & Niv, 2015). First, we infer the properties of each action from the action observations given as prior knowledge. Second, a policy learns to make decisions based on these inferred action properties. When a new action set is given, their properties are inferred and exploited by the policy to solve the task. Formally, we propose a two-stage framework:

- 1. Learning Action Representations:** We use unsupervised representation learning to encode each set of action observations into an action representation. This representation expresses the latent action properties present in the set of diverse observations (Section 4.1).
- 2. Learning Generalizable Policy:** We propose a flexible policy architecture to incorporate action representations as inputs, which can be trained through RL (Section 4.2). We provide a training procedure to control overfitting to the training action set, making the policy generalize better to unseen actions (Section 4.3).

4.1. Unsupervised Learning of Action Representations

Our goal is to encode each set of action observations into an action representation that can be used by a policy to make decisions in a task. The main challenge is to extract the shared statistics of the action’s behavior from high-dimensional and diverse observations.

To address this, we employ the hierarchical variational autoencoder (HVAE) by Edwards & Storkey (2017). HVAE first summarizes the entire set of an action’s observations into a single action latent. This action latent then conditions the encoding and reconstruction of each constituent observation through a conditional VAE. Such hierarchical

conditioning ensures that the observations for the same action are organized together in the latent space. Furthermore, the action latent sufficiently encodes the diverse statistics of the action. Therefore, this action latent is used as the action’s representation in the downstream RL task (Figure 2).

Formally, for each training action $a_i \in \mathbb{A}$, HVAE encodes its associated action observations $\mathcal{O}_i \in \mathbb{O}$ into a representation c_i by mean-pooling over the individual observations $o_{i,j} \in \mathcal{O}_i$. We refer to this action encoder as the action representation module $q_\phi(c_i|\mathcal{O}_i)$. The action latent c_i sampled from the action encoder is used to condition the encoders $q_\psi(z_{i,j}|o_{i,j}, c_i)$ and decoders $p(o_{i,j}|z_{i,j}, c_i)$ for each individual observation $o_{i,j} \in \mathcal{O}_i$. The entire HVAE framework is trained with reconstruction loss across the individual observations, along with KL-divergence regularization of encoders q_ϕ and q_ψ with their respective prior distributions $p(c)$ and $p(z|c_i)$. For additional details on HVAE, refer to Appendix D.3.1 and Edwards & Storkey (2017). The final training objective requires maximizing the ELBO:

$$\mathcal{L} = \sum_{\mathcal{O} \in \mathbb{O}} \left[\mathbb{E}_{q_\phi(c|\mathcal{O})} \left[\sum_{o \in \mathcal{O}} \mathbb{E}_{q_\psi(z|o,c)} \log p(o|z,c) - D_{KL}(q_\psi||p(z|c)) \right] - D_{KL}(q_\phi||p(c)) \right]. \quad (2)$$

For action observations consisting of sequential data, $o = \{x_0, \dots, x_m\}$ like state trajectories or videos, we augment HVAE to extract temporally extended behaviors of actions. We accomplish this by incorporating insights from trajectory autoencoders (Wang et al., 2017; Co-Reyes et al., 2018) in HVAE. Bi-LSTM (Schuster & Paliwal, 1997) is used in the encoders and LSTM is used as the decoder $p(x_1, \dots, x_m|z, c, x_0)$ to reconstruct the trajectory given the initial state x_0 . Explicitly for video observations, we also incorporated temporal skip connections (Ebert et al., 2017) by predicting an extra mask channel to balance contributions from the predicted and first frame of the video.

We set the representation for an action as the mean of the inferred distribution $q_\phi(c_i|\mathcal{O}_i)$ as done in Higgins et al. (2017a); Steenbrugge et al. (2018).

4.2. Adaptable Policy Architecture

To enable decision-making with new actions, we develop a policy architecture that can adapt to any available action set \mathcal{A} by taking the list of action representations as input. Since the action representations are learned independently of the downstream task, a task-solving policy must learn to extract the relevant task-specific knowledge.

The policy $\pi(a|s, \mathcal{A})$ receives a set of available actions $\mathcal{A} = \{a_1, \dots, a_k\}$ as input, along with the action representations $\{c_1, \dots, c_k\}$. As shown in Figure 2, the policy architecture starts with a state encoder f_ω . The utility

Algorithm 1. Two-stage Training Framework

- 1: **Inputs:** Training actions \mathbb{A} , action observations \mathbb{O}
 - 2: Randomly initialize HVAE and policy parameters
 - 3: **for** epoch = 1, 2, ... **do**
 - 4: Sample batch of action observations $\mathcal{O}_i \sim \mathbb{O}$
 - 5: Train HVAE parameters with gradient ascent on Eq. 2
 - 6: **end for**
 - 7: Infer action representations: $c_i = q_\phi^\mu(\mathcal{O}_i), \forall a_i \in \mathbb{A}$
 - 8: **for** iteration = 1, 2, ... **do**
 - 9: **while** episode not done **do**
 - 10: Subsample action set $\mathcal{A} \subset \mathbb{A}$ of size m
 - 11: Sample action $a_t \sim \pi_\theta(s, \mathcal{A})$ using Eq. 3
 - 12: $s_{t+1}, r_t \leftarrow \text{ENV}(s_t, a_t)$
 - 13: Store experience (s_t, a_t, s_{t+1}, r_t) in replay buffer
 - 14: **end while**
 - 15: Update and save policy θ using PPO on Eq. 4
 - 16: **end for**
 - 17: Select θ with best validation performance
-

Algorithm 2. Generalization to New Actions

- 1: **Inputs:** New actions $\mathcal{A} = \{a_1, \dots, a_M\}$, observations $\{\mathcal{O}_1, \dots, \mathcal{O}_M\}$. Trained networks q_ϕ and π_θ
 - 2: Infer action representations: $c_i = q_\phi^\mu(\mathcal{O}_i), \forall a_i \in \mathcal{A}$
 - 3: **while** not done **do**
 - 4: Sample action $a_t \sim \pi_\theta(s, \mathcal{A})$ using Eq. 3
 - 5: $s_{t+1}, r_t \leftarrow \text{ENV}(s_t, a_t)$
 - 6: **end while**
-

function f_ν is applied to each given action’s representation c_i and the encoded state $f_\omega(s)$ (Eq. 3). The utility function estimates the score of an action at the current state, through its action representation, just like a Q-function (Watkins & Dayan, 1992). Action utility scores are converted into a probability distribution through a softmax function:

$$\pi(a_i|s, \mathcal{A}) = \frac{e^{f_\nu[c_i, f_\omega(s)]}}{\sum_{j=1}^k e^{f_\nu[c_j, f_\omega(s)]}}. \quad (3)$$

In many physical environments, the choice of a discrete action is associated with auxiliary parameterizations, such as the intended position of tool usage or a binary variable to determine episode termination. We incorporate such hybrid action spaces (Hausknecht & Stone, 2015), through an auxiliary network f_χ , which takes the encoded state and outputs a distribution over the auxiliary actions¹. An environment action is taken by sampling the auxiliary action from this distribution and the discrete action from Eq. 3. The policy parameters $\theta = \{\nu, \omega, \chi\}$ are trained end-to-end using policy gradients (Sutton et al., 2000).

¹Alternatively, the auxiliary network can take the discrete selection as input as tested in Appendix C.4

4.3. Generalization Objective and Training Procedure

Our final objective is to find policy parameters θ to maximize reward on held-out action sets $\mathcal{A} \subset \mathbb{A}'$ (Eq. 1), while being trained on a limited set of actions \mathbb{A} . We study this generalization problem based on statistical learning theory (Vapnik, 1998; 2013) in supervised learning. Particularly, generalization of machine learning models is expected when their training inputs are independent and identically distributed (Bousquet et al., 2003). However, in RL, a policy typically acts in the environment to collect its own training data. Thus when a policy overexploits a specific subset of the training actions, this skews the policy training data towards those actions. To avoid this form of overfitting and be robust to diverse new action sets, we propose the following regularizations to approximate i.i.d. training:

- **Subsampled action spaces:** To limit the actions available in each episode of training, we randomly subsample action sets, $\mathcal{A} \subset \mathbb{A}$ of size m , a hyperparameter. This avoids overfitting to any specific actions by forcing the policy to solve the task with diverse action sets.
- **Maximum entropy regularization:** We further diversify the policy’s actions during training using the maximum entropy objective (Ziebart et al., 2008). We add the entropy of the policy $\mathcal{H}[\pi_\theta(a|s)]$ to the RL objective with a hyperparameter weighting β . While this objective has been widely used for exploration, we find it useful to enable generalization to new actions.
- **Validation-based model selection:** During training, the models are evaluated on held-out validation sets of actions, and the best performing model is selected. Just like supervised learning, this helps to avoid overfitting the policy during training. Note that the validation set is also used to tune hyperparameters such as entropy coefficient β and subsampled action set size m . There is no overlap between test and validation sets, hence the test actions are still completely unseen at evaluation.

The final policy training objective is:

$$\max_{\theta} \mathbb{E}_{\mathcal{A} \subset \mathbb{A}, a \sim \pi_\theta(\cdot|s, \mathcal{A})} [R(s) + \beta \mathcal{H}[\pi_\theta(a|s, \mathcal{A})]]. \quad (4)$$

The training procedure is described in Algorithm 1. The HVAE is trained using RAdam optimizer (Liu et al., 2019), and we use PPO (Schulman et al., 2017) to train the policy with Adam Optimizer (Kingma & Ba, 2015). Additional implementation and experimental details, including the hyperparameters searched, are provided in Appendix D. The inference process is described in Algorithm 2. When given a new set of actions, we can infer the action representations with the trained HVAE module. The policy can also generalize to utilize these actions since it has learned to map a list of action representations to an action probability distribution.

5. Experimental Setup

5.1. Environments

We propose four sequential decision-making environments with diverse actions to evaluate and benchmark the proposed problem of generalization to new actions. These test the action representation learning method on various types of action observations. The long-horizon nature of the environments presents a challenge to use new actions correctly to solve the given tasks consistently. Figure 3 provides an overview of the task, types of actions, and action observations in three environments. In each environment, the train-test-validation split is approximately 50-25-25%. Complete details on each environment, action observations, and train-validation-test splits can be found in Appendix A.

5.1.1. GRID WORLD

In the Grid world environment (Chevalier-Boisvert et al., 2018), an agent navigates a 2D lava maze to reach a goal using predefined skills. Each skill is composed of a 5-length sequence of left, right, up or down movement. The total number of available skills is 4^5 . Action observations consist of state sequences of an agent observed by applying the skill in an empty grid. This environment acts as a simple demonstration of generalization to unseen skill sets.

5.1.2. RECOMMENDER SYSTEM

The Recommender System environment (Rohde et al., 2018) simulates users responding to product recommendations. Every episode, the agent makes a series of recommendations for a new user to maximize their click-through rate (CTR). With a total of 10,000 products as actions, the agent is evaluated on how well it can recommend previously unseen products to users. The environment specifies predefined action representations. Thus we only evaluate our policy framework on it, not the action encoder.

5.1.3. CREATE

We develop the Chain REAction Tool Environment (CREATE) as a challenging benchmark to test generalization to new actions². It is a physics-based puzzle where the agent must place tools in real-time to manipulate a specified ball’s trajectory to reach a goal position (Figure 3). The environment features 12 different tasks and 2,111 distinct tools. Moreover, it tests physical reasoning since every action involves selecting a tool and predicting the 2D placement for it, making it a hybrid action-space environment. Action observations for a tool consist of a test ball’s trajectories interacting with the tool from various directions and speeds. CREATE tasks evaluate the ability to understand complex

²CREATE environment: <https://clvr.ai/create>

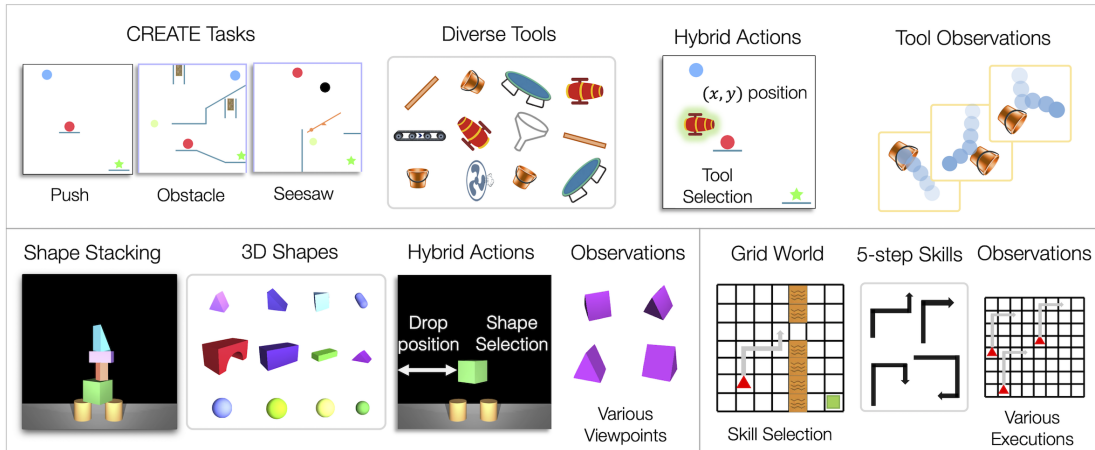


Figure 3. Benchmark environments for evaluating generalization to new actions. (Top) In CREATE, an agent selects and places various tools to move the red ball to the goal. Other moving objects can serve as help or obstacles. Some tasks also have subgoals to help with exploration (Appendix C.3 shows results with no subgoal rewards). The tool observations consist of trajectories of a test ball interacting with the tool. (Left) In Shape Stacking, an agent selects and places 3D shapes to stack a tower. The shape observations are images of the shape from different viewpoints. (Right) In Grid World, an agent reaches the goal by choosing from 5-step navigation skills. The skill observations are collected on an empty grid in the form of agent trajectories resulting from skill execution from random locations.

functionalities of unseen tools and utilize them for various tasks. We benchmark our framework on all 12 CREATE tasks with the extended results in Appendix C.1.

5.1.4. SHAPE STACKING

We develop a MuJoCo-based (Todorov et al., 2012) Shape Stacking environment, where the agent drops blocks of different shapes to build a tall and stable tower. Like in CREATE, the discrete selection of shape is parameterized by the coordinates of where to place the selected shape and a binary action to decide whether to stop stacking. This environment evaluates the ability to use unseen complex 3D shapes in a long horizon task and contains 810 shapes.

5.2. Experiment Procedure

We perform the following procedure for each action generalization experiment³.

1. *Collect action observations* for all the actions using a supplemental play environment that is task-independent.
2. *Split the actions* into train, validation, and test sets.
3. *Train HVAE* on the train action set by autoencoding the collected action observations.
4. *Infer action representations* for all the actions using the trained HVAE encoder on their action observations.
5. *Train policy* on the task environment with RL. In each episode, an action set is randomly sampled from the train actions. The policy acts by using the list of inferred

action representations as input.

6. **Evaluation:** In each episode, an action set is subsampled from the test (or validation) action set. The trained policy uses the inferred representations of these actions to act in the environment zero-shot. The performance metric (e.g. success rate) is averaged over multiple such episodes.
 - (a) Perform hyperparameter tuning and model selection by evaluating on the *validation action set*.
 - (b) Report final performance on the *test action set*.

5.3. Baselines

We validate the design choices of the proposed action encoder and policy architecture. For action encoder, we compare with a policy using action representations from a non-hierarchical encoder. For policy architecture, we consider alternatives that select actions using distances in the action representation space instead of learning a utility function.

- **Non-hierarchical VAE:** A flat VAE is trained over the individual action observations. An action’s representation is taken as the mean of encodings of the constituent action observations.
- **Continuous-output:** The policy architecture outputs a continuous vector in the action representation space, following Dulac-Arnold et al. (2015). From any given action set, the action closest to this output is selected.
- **Nearest-Neighbor:** A standard discrete action policy is trained. The representation of this policy’s output action is used to select the nearest neighbor from new actions.

³Complete code available at <https://github.com/clvrai/new-actions-rl>

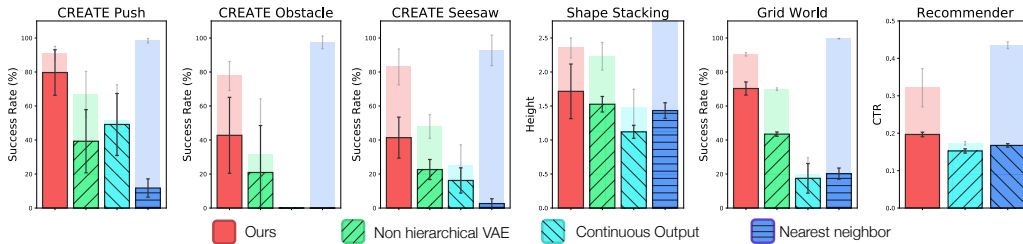


Figure 4. Comparison against baseline action representation and policy architectures on 6 environments, 3 of which are CREATE tasks. The solid bar denotes the test performance and the transparent bar the training performance, to observe the generalization gap. The results are averaged over 5000 episodes across 5 random seeds, and the error bars indicate the standard deviation (8 seeds for Grid World). All learning curves are present in Figure 24. Results on 9 additional CREATE tasks can be found in Appendix C.1.

5.4. Ablations

We individually ablate the two proposed regularizations:

- **Ours without subsampling:** Trained over the entire set of training actions without any action space sampling.
- **Ours without entropy:** Trained without entropy regularization, by setting the entropy coefficient to zero.

6. Results and Analysis

Our experiments aim to answer the following questions about the proposed problem and framework: (1) Can the HVAE extract meaningful action characteristics from the action observations? (2) What are the contributions of the proposed action encoder, policy architecture, and regularizations for generalization to new actions? (3) How well does our framework generalize to varying difficulties of test actions and types of action observations? (4) How inefficient is finetuning to a new action space as compared to zero-shot generalization?

6.1. Visualization of Inferred Action Representations

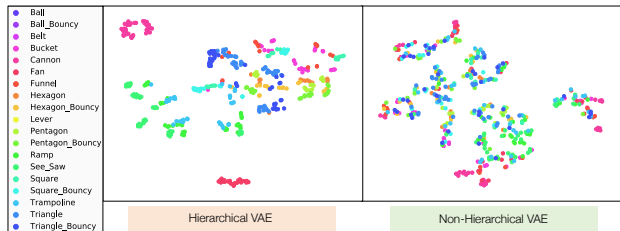


Figure 5. t-SNE visualization of action representations for held-out tools in CREATE inferred using a trained HVAE (left) and a VAE (right). The color indicates the tool class (e.g. cannons, buckets). The HVAE encoder learns to organize semantically similar tools together, in contrast to the flat VAE, which shows less structure.

To investigate if the HVAE can extract important characteristics from observations of new actions, we visualize the inferred action representations for unseen CREATE tools. In Figure 5, we observe that tools from the same class are

clustered together in the HVAE representations. Whereas in the absence of hierarchy, the action representations are less organized. This shows that encoding action observations independently, and averaging them to obtain a representation can result in the loss of semantic information, such as the tool’s class. In contrast, hierarchical conditioning on action representation enforces various constituent observations to be encoded together. This helps to model the diverse statistics of the action’s observations into its representation.

6.2. Results and Comparisons

6.2.1. BASELINES

Figure 4 shows that our framework outperforms the baselines (Section 5.3) in zero-shot generalization to new actions on six tasks. The non-hierarchical VAE baseline has lower policy performance in both training and testing. This shows that HVAE extracts better representations from action observations that facilitate easier policy learning.

The continuous-output baseline suffers in training as well as testing performance. This is likely due to the complex task of indirect action selection. The distance metric used to find the closest action does not directly correspond to the task relevance. Therefore the policy network must learn to adjust its continuous output, such that the desired discrete action ends up closest to it. Our method alleviates this through the utility function, which first extracts task-relevant features to enable an appropriate action decision. The nearest-neighbor baseline achieves high training performance since it is merely discrete-action RL with a fixed action set. However, at test time, the simple nearest-neighbor in action representation space does not correspond to the actions’ task-relevance. This results in poor generalization performance.

6.2.2. ABLATIONS

Figure 6 assesses the contribution of the proposed regularizations to avoid overfitting to training actions. Entropy regularization usually leads to better training and test performance due to better exploration. In the recommender envi-

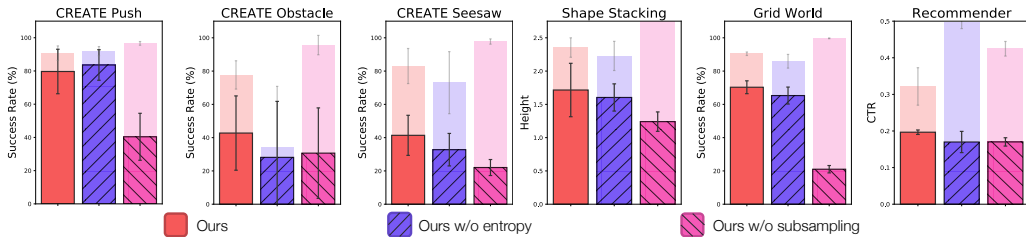
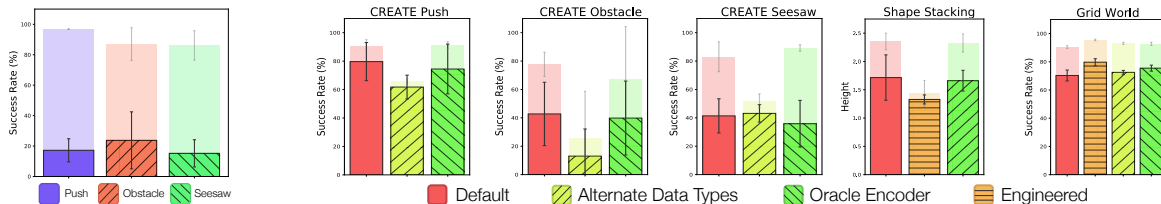


Figure 6. Analyzing the importance of the proposed action space subsampling and entropy regularization in our method. The training and evaluation details are the same as Figure 4.



(a) Unseen tool classes in CREATE

(b) Alternate action representations

Figure 7. Additional analyses. (a) Our method achieves decent performance on out-of-distribution tools in 3 CREATE tasks, but the generalization gap is more pronounced. (b) Various action representations can be successfully used with our policy architecture.

ronment, the generalization gap is more substantial without entropy regularization. Without any incentive to diversify, the policy achieved high training performance by overfitting to certain products. We observe a similar effect in the absence of action subsampling across all tasks. It achieves a higher training performance, due to the ease of training in non-varying action space. However, its generalization performance is weak because it is easy to overfit when the policy has access to all the actions during training.

6.3. Analyzing the Limits of Generalization

6.3.1. GENERALIZATION TO UNSEEN ACTION CLASSES

Our method is expected to generalize when new actions are within the distribution of those seen during training. However, what happens when we test our approach on completely unseen action classes? Generalization is still expected because the characteristic action observations enable the representation of actions in the same space. Figure 7a evaluates our approach on held-out tool classes in the CREATE environment. Some tool classes like trampolines and cannons are only seen during training, whereas others like fans and conveyor belts are only used during testing. While the generalization gap is more substantial than before, we still observe reasonable task success across the 3 CREATE tasks. The performance can be further improved by increasing the size and diversity of training actions. Appendix C.6 shows a similar experiment on Shape Stacking.

6.3.2. ALTERNATE ACTION REPRESENTATIONS

In Figure 7b, we study policy performance for various action representations. See Appendix B for t-SNE visualizations.

- **Alternate Data Types** of action observations are used to learn representations. For CREATE, we use video data instead of the state trajectory of the test ball (see Figure 3). For Grid World, we test with a one-hot vector of agent location instead of (x, y) coordinates. The policy performance using these representations is comparable to the default. This shows that HVAE is suitable for high-dimensional action observations, such as videos.
- **Oracle HVAE** is used to get representations by training on the test actions. The performance difference between default and oracle HVAE is negligible. This shows that HVAE generalizes well to unseen action observations.
- **Hand-Engineered** action representations are used for Stacking and Grid World, by exploiting ground-truth information about the actions. In Stacking, HVAE outperforms these representations, since it is hard to specify the information about shape geometry manually. In contrast, it is easy to specify the complete skill in Grid World. Nevertheless, HVAE representations perform comparably.

6.3.3. VARYING THE DIFFICULTY OF GENERALIZATION

Figure 9 shows a detailed study of generalization on various degrees of differences between the train and test actions in 3 CREATE tasks. We vary the following parameters:

- Tool Angle:** Each sampled test tool is at least θ degrees different from the most similar tool seen during training.
- Tool Embedding:** Each test tool’s representation is at least d Euclidean distance away from each training tool.
- Unseen Ratio:** The test action set is a mixture of seen and unseen tools, with $x\%$ unseen.

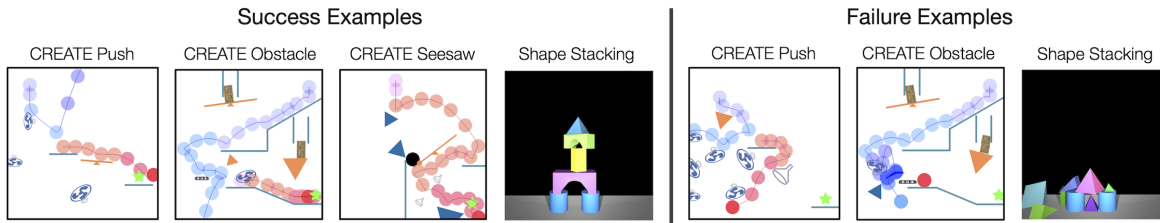
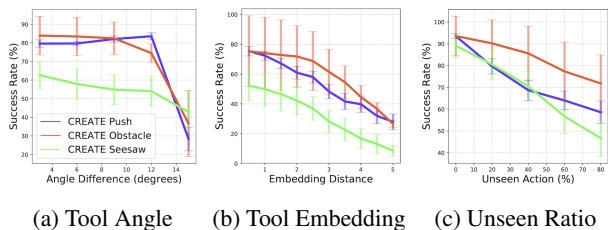


Figure 8. Evaluation results showing the trajectories of objects in CREATE and the final tower in Shape Stacking. Our framework is generally able to infer the dynamic properties of tools and geometry of shapes and subsequently use them to make the right decisions.



(a) Tool Angle (b) Tool Embedding (c) Unseen Ratio
 Figure 9. Varying the test action space. An increasing x-axis corresponds to more difficult generalization conditions. Each value plotted is the average test performance over 5 random seeds with the error bar corresponding to the standard deviation.

The results suggest a gradual decrease in generalization performance as the test actions become more different from training actions. We chose the hardest settings for the main experiments: 15° angle difference and 100% unseen actions.

6.3.4. QUALITATIVE ANALYSIS

Figure 8 shows success and failure examples when using unseen actions in the CREATE and Stacking environments. In CREATE, our framework correctly infers the directional pushing properties of unseen tools like conveyor belts and fans from their action observations and can utilize them to solve the task. Failure examples include placements being off and misrepresenting the direction of a belt. Collecting more action observations can improve the representations.

In Shape Stacking, the geometric properties of 3D shapes are correctly inferred from image action observations. The policy can act in the environment by selecting the appropriate shapes to drop based on the current tower height. Failures include greedily selecting a tall but unstable shape in the beginning, like a pyramid.

6.4. The Inefficiency of Finetuning on New Actions

In Figure 10, we examine various approaches to continue training on a particular set of new actions in CREATE Push. First, we train a policy from scratch on the new actions either with our adaptable policy architecture (Ours Scratch) or a regular discrete policy (Discrete Scratch). These take around 3 million environment steps to achieve our pretrained method’s zero-shot performance (Ours Zero-Shot). Next, we consider ways to transfer knowledge from training actions. We train a regular discrete policy and finetune on new

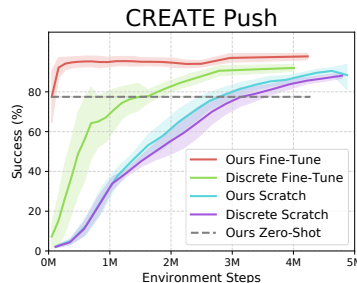


Figure 10. Finetuning or training policies from scratch on the new action space. The horizontal line is the zero-shot performance of our method. Each line is the average test performance over 5 random seeds, while the shaded region is the standard deviation.

actions by re-initializing the final layer (Discrete Fine-Tune). While this approach transfers some task knowledge, it disregards any relationship between the old and new actions. It still takes over 1 million steps to reach our zero-shot performance. This shows how expensive retraining is on a single action set. Clearly, this retraining process is prohibitive in scenarios where the action space frequently changes. This demonstrates the significance of addressing the problem of zero-shot generalization to new actions. Finally, we continue training our pretrained policy on the new action set with RL (Ours Fine-Tune). We observe fast convergence to optimal performance, because of its ability to utilize action representations to transfer knowledge from the training actions to the new actions. Finetuning results for all other environments are in Figure 19.

7. Conclusion

Generalization to novel circumstances is vital for robust agents. We propose the problem of enabling RL policies to generalize to new action spaces. Our two-stage framework learns action representations from acquired action observations and utilizes them to make the downstream RL policy flexible. We propose four challenging benchmark environments and demonstrate the efficacy of hierarchical representation learning, policy architecture, and regularizations. Exciting directions for future research include building general problem-solving agents that can adapt to new tasks with new action spaces, and autonomously acquiring informative action observations in the physical world.

Acknowledgements

This project was funded by SKT. The authors are grateful to Youngwoon Lee and Jincheng Zhou for help with RL experiments and writing. The authors would like to thank Shao-Hua Sun, Karl Pertsch, Dweep Trivedi and many members of the USC CLVR lab for fruitful discussions. The authors appreciate the feedback from anonymous reviewers who helped improve the paper.

References

- Allen, K. R., Smith, K. A., and Tenenbaum, J. B. The tools challenge: Rapid trial-and-error learning in physical problem solving. *arXiv preprint arXiv:1907.09620*, 2019. 14
- Andreas, J., Klein, D., and Levine, S. Modular multitask reinforcement learning with policy sketches. In *International Conference on Machine Learning*, pp. 166–175, 2017. 2
- Bakhtin, A., van der Maaten, L., Johnson, J., Gustafson, L., and Girshick, R. Phyre: A new benchmark for physical reasoning. *arXiv:1908.05656*, 2019. 14
- Bengio, Y., Courville, A., and Vincent, P. Representation learning: A review and new perspectives. *IEEE transactions on pattern analysis and machine intelligence*, 35(8): 1798–1828, 2013. 2
- Biewald, L. Experiment tracking with weights and biases, 2020. URL <https://www.wandb.com/>. Software available from wandb.com. 20
- Blomqvist, V. Pymunk. URL <http://www.pymunk.org/>. Accessed 2020-02-18. 14
- Bousquet, O., Boucheron, S., and Lugosi, G. Introduction to statistical learning theory. In *Summer School on Machine Learning*, pp. 169–207. Springer, 2003. 5, 20
- Brockman, G., Cheung, V., Pettersson, L., Schneider, J., Schulman, J., Tang, J., and Zaremba, W. Openai gym. *arXiv preprint arXiv:1606.01540*, 2016. 20
- Chandak, Y., Theodorou, G., Kostas, J., Jordan, S., and Thomas, P. S. Learning action representations for reinforcement learning. *arXiv preprint arXiv:1902.00183*, 2019. 2
- Chandak, Y., Theodorou, G., Nota, C., and Thomas, P. Lifelong learning with a changing action set. *Proceedings of the AAAI Conference on Artificial Intelligence*, 34(04):3373–3380, Apr 2020. ISSN 2159-5399. doi: 10.1609/aaai.v34i04.5739. URL <http://dx.doi.org/10.1609/aaai.v34i04.5739>. 2
- Chen, Y., Chen, Y., Yang, Y., Li, Y., Yin, J., and Fan, C. Learning action-transferable policy with action embedding. *arXiv preprint arXiv:1909.02291*, 2019. 2
- Chevalier-Boisvert, M., Willems, L., and Pal, S. Minimalistic gridworld environment for openai gym. <https://github.com/maximecb/gym-minigrid>, 2018. 5, 13
- Chou, P.-W., Maturana, D., and Scherer, S. Improving stochastic policy gradients in continuous control with deep reinforcement learning using the beta distribution. In *International Conference on Machine Learning*, pp. 834–843, 2017. 22
- Co-Reyes, J., Liu, Y., Gupta, A., Eysenbach, B., Abbeel, P., and Levine, S. Self-consistent trajectory autoencoder: Hierarchical reinforcement learning with trajectory embeddings. In *International Conference on Machine Learning*, pp. 1008–1017, 2018. 4
- Cobbe, K., Klimov, O., Hesse, C., Kim, T., and Schulman, J. Quantifying generalization in reinforcement learning. *arXiv preprint arXiv:1812.02341*, 2018. 1, 2
- Denton, E. L. and Birodkar, v. Unsupervised learning of disentangled representations from video. In Guyon, I., Luxburg, U. V., Bengio, S., Wallach, H., Fergus, R., Vishwanathan, S., and Garnett, R. (eds.), *Advances in Neural Information Processing Systems 30*, pp. 4414–4423. Curran Associates, Inc., 2017. URL <http://papers.nips.cc/paper/7028-unsupervised-learning-of-disentangled-representations-from-video.pdf>. 2
- Dulac-Arnold, G., Evans, R., van Hasselt, H., Sunehag, P., Lillicrap, T., Hunt, J., Mann, T., Weber, T., Degris, T., and Coppin, B. Deep reinforcement learning in large discrete action spaces. *arXiv preprint arXiv:1512.07679*, 2015. 2, 6
- Ebert, F., Finn, C., Lee, A. X., and Levine, S. Self-supervised visual planning with temporal skip connections. In *Conference on Robot Learning*, pp. 344–356, 2017. 4, 22
- Edwards, H. and Storkey, A. Towards a neural statistician. In *International Conference on Learning Representations*, 2017. URL <https://openreview.net/forum?id=HJDBUF51e>. 2, 3, 4, 21
- Fang, K., Zhu, Y., Garg, A., Kurenkov, A., Mehta, V., Fei-Fei, L., and Savarese, S. Learning task-oriented grasping for tool manipulation from simulated self-supervision. *arXiv preprint arXiv:1806.09266*, 2018. 2

- Finn, C., Abbeel, P., and Levine, S. Model-agnostic meta-learning for fast adaptation of deep networks. In *International Conference on Machine Learning*, pp. 1126–1135, 2017. 1
- Gershman, S. J. and Niv, Y. Novelty and inductive generalization in human reinforcement learning. *Topics in cognitive science*, 7(3):391–415, 2015. 3
- Hausknecht, M. and Stone, P. Deep reinforcement learning in parameterized action space. *arXiv preprint arXiv:1511.04143*, 2015. 4
- Hawkins, D. M. The problem of overfitting. *Journal of chemical information and computer sciences*, 44(1):1–12, 2004. 2
- He, J., Chen, J., He, X., Gao, J., Li, L., Deng, L., and Ostendorf, M. Deep reinforcement learning with a natural language action space. *arXiv preprint arXiv:1511.04636*, 2015. 2
- Higgins, I., Matthey, L., Pal, A., Burgess, C., Glorot, X., Botvinick, M., Mohamed, S., and Lerchner, A. beta-vae: Learning basic visual concepts with a constrained variational framework. *ICLR*, 2(5):6, 2017a. 4
- Higgins, I., Pal, A., Rusu, A., Matthey, L., Burgess, C., Pritzel, A., Botvinick, M., Blundell, C., and Lerchner, A. Darla: Improving zero-shot transfer in reinforcement learning. In *Proceedings of the 34th International Conference on Machine Learning-Volume 70*, pp. 1480–1490. JMLR. org, 2017b. 2
- Ioffe, S. and Szegedy, C. Batch normalization: Accelerating deep network training by reducing internal covariate shift. *arXiv preprint arXiv:1502.03167*, 2015. 21
- Kim, H., Kim, J., Jeong, Y., Levine, S., and Song, H. O. EMI: Exploration with mutual information. In Chaudhuri, K. and Salakhutdinov, R. (eds.), *Proceedings of the 36th International Conference on Machine Learning*, volume 97 of *Proceedings of Machine Learning Research*, pp. 3360–3369, Long Beach, California, USA, 09–15 Jun 2019. PMLR. URL <http://proceedings.mlr.press/v97/kim19a.html>. 2
- Kingma, D. P. and Ba, J. Adam: A method for stochastic optimization. In *International Conference on Learning Representations*, 2015. 5, 21
- Kostrikov, I. Pytorch implementations of reinforcement learning algorithms. <https://github.com/ikostrikov/pytorch-a2c-ppo-acktr-gail>, 2018. 21
- Laversanne-Finot, A., Pere, A., and Oudeyer, P.-Y. Curiosity driven exploration of learned disentangled goal spaces. In Billard, A., Dragan, A., Peters, J., and Morimoto, J. (eds.), *Proceedings of The 2nd Conference on Robot Learning*, volume 87 of *Proceedings of Machine Learning Research*, pp. 487–504. PMLR, 29–31 Oct 2018. URL <http://proceedings.mlr.press/v87/laversanne-finot18a.html>. 2
- Legg, S. and Hutter, M. Universal intelligence: A definition of machine intelligence. *Minds and machines*, 17(4): 391–444, 2007.
- Liu, L., Jiang, H., He, P., Chen, W., Liu, X., Gao, J., and Han, J. On the variance of the adaptive learning rate and beyond. *arXiv preprint arXiv:1908.03265*, 2019. 5, 21
- Nair, A. V., Pong, V., Dalal, M., Bahl, S., Lin, S., and Levine, S. Visual reinforcement learning with imagined goals. In *Advances in Neural Information Processing Systems*, pp. 9191–9200, 2018. 2
- Nichol, A., Pfau, V., Hesse, C., Klimov, O., and Schulman, J. Gotta learn fast: A new benchmark for generalization in rl. *arXiv preprint arXiv:1804.03720*, 2018. 1, 2
- Oh, J., Singh, S., Lee, H., and Kohli, P. Zero-shot task generalization with multi-task deep reinforcement learning. In *International Conference on Machine Learning*, pp. 2661–2670, 2017. 2
- Packer, C., Gao, K., Kos, J., Krähenbühl, P., Koltun, V., and Song, D. Assessing generalization in deep reinforcement learning. *arXiv preprint arXiv:1810.12282*, 2018. 2
- Parisi, G. I., Kemker, R., Part, J. L., Kanan, C., and Wermter, S. Continual lifelong learning with neural networks: A review. *arXiv preprint arXiv:1802.07569*, 2018. 1
- Paszke, A., Gross, S., Chintala, S., Chanan, G., Yang, E., DeVito, Z., Lin, Z., Desmaison, A., Antiga, L., and Lerer, A. Automatic differentiation in PyTorch. In *NIPS Autodiff Workshop*, 2017. 20
- Pathak, D., Lu, C., Darrell, T., Isola, P., and Efros, A. A. Learning to control self-assembling morphologies: A study of generalization via modularity. In *arXiv preprint arXiv:1902.05546*, 2019. 1, 2
- Rohde, D., Bonner, S., Dunlop, T., Vasile, F., and Karatzoglou, A. Recogym: A reinforcement learning environment for the problem of product recommendation in online advertising. *arXiv preprint arXiv:1808.00720*, 2018. 5, 13, 14
- Sanchez-Gonzalez, A., Heess, N., Springenberg, J. T., Merel, J., Riedmiller, M., Hadsell, R., and Battaglia, P. Graph networks as learnable physics engines for inference and control. In *International Conference on Machine Learning*, 2018. 2

- Schulman, J., Wolski, F., Dhariwal, P., Radford, A., and Klimov, O. Proximal policy optimization algorithms. *arXiv preprint arXiv:1707.06347*, 2017. 5, 21
- Schuster, M. and Paliwal, K. K. Bidirectional recurrent neural networks. *IEEE Transactions on Signal Processing*, 45(11):2673–2681, 1997. 4
- Shinners, P. Pygame. URL <http://pygame.org/>. Accessed 2020-02-18. 14
- Steenbrugge, X., Leroux, S., Verbelen, T., and Dhoedt, B. Improving generalization for abstract reasoning tasks using disentangled feature representations. *arXiv preprint arXiv:1811.04784*, 2018. 2, 4
- Sutton, R. S., McAllester, D. A., Singh, S. P., and Mansour, Y. Policy gradient methods for reinforcement learning with function approximation. In *Advances in neural information processing systems*, pp. 1057–1063, 2000. 4
- Tennenholtz, G. and Mannor, S. The natural language of actions. *arXiv preprint arXiv:1902.01119*, 2019. 2
- Todorov, E., Erez, T., and Tassa, Y. Mujoco: A physics engine for model-based control. In *2012 IEEE/RSJ International Conference on Intelligent Robots and Systems*, pp. 5026–5033. IEEE, 2012. 6
- Vapnik, V. *Statistical learning theory*, 1998. 5
- Vapnik, V. *The nature of statistical learning theory*. Springer science & business media, 2013. 5
- Wang, T., Liao, R., Ba, J., and Fidler, S. Nervenet: Learning structured policy with graph neural networks. In *International Conference on Learning Representations*, 2018. URL <https://openreview.net/forum?id=S1sqHMZCb>. 1, 2
- Wang, Z., Merel, J. S., Reed, S. E., de Freitas, N., Wayne, G., and Heess, N. Robust imitation of diverse behaviors. In Guyon, I., Luxburg, U. V., Bengio, S., Wallach, H., Fergus, R., Vishwanathan, S., and Garnett, R. (eds.), *Advances in Neural Information Processing Systems 30*, pp. 5320–5329. Curran Associates, Inc., 2017. URL <http://papers.nips.cc/paper/7116-robust-imitation-of-diverse-behaviors.pdf>. 4
- Watkins, C. J. and Dayan, P. Q-learning. *Machine learning*, 8(3-4):279–292, 1992. 4
- Xie, A., Ebert, F., Levine, S., and Finn, C. Improvisation through physical understanding: Using novel objects as tools with visual foresight, 2019. 2
- Xu, D., Nair, S., Zhu, Y., Gao, J., Garg, A., Fei-Fei, L., and Savarese, S. Neural task programming: Learning to generalize across hierarchical tasks. In *International Conference on Robotics and Automation*, 2017. 2
- Ziebart, B. D., Maas, A., Bagnell, J. A., and Dey, A. K. Maximum entropy inverse reinforcement learning. In *Proceedings of the 23rd national conference on Artificial intelligence-Volume 3*, pp. 1433–1438. AAAI Press, 2008. 5

Generalization to New Actions in Reinforcement Learning - Appendix

A. Environment Details

A.1. Grid World

The Grid World environment, based on [Chevalier-Boisvert et al. \(2018\)](#), consists of an agent and a randomly placed lava wall with an opening, as shown in Figure 11. The lava wall can either be horizontal or vertical. The agent spawns in the top left corner, and its objective is to reach the goal in the bottom-right corner of the grid while avoiding any path through lava. The agent can move using 5-step skills composed of steps in one of the four directions (Up, Down, Left, and Right). An episode is terminated when the agent uses a maximum of 10 actions (50 moves), or the agent reaches the goal (success) or lava wall (failure).

State: The state space is a flattened version of the 9x9 grid. Each element of the 81-dimensional state contains an integer ID based on whether the cell is empty, wall, agent, goal, lava, or subgoal.

Actions: An action or skill of the agent is a sequence of 5 consecutive moves in 4 directions. Hence, $4^5 = 1,024$ total actions are possible. Once the agent selects an action, it executes 5 sequential moves step-by-step. During a skill execution, if the agent hits the boundary wall, it will stay in the current cell, making a null interaction. If the agent steps on lava during any action, the game will be terminated.

Reward: Grid world provides a sparse subgoal reward on passing the subgoal for the first time and a sparse goal reward when the agent reaches the goal. The goal reward is discounted based on the number of actions taken to encourage a shorter path to the goal. More concretely,

$$R(s) = \lambda_{Subgoal} \cdot \mathbf{1}_{Subgoal} + (1 - \lambda_{Goal} \frac{N_{total}}{N_{max}}) \cdot \mathbf{1}_{Goal} \quad (5)$$

where $\lambda_{Subgoal} = 0.1$, $\lambda_{Goal} = 0.9$, $N_{max} = 50$, N_{total} = number of moves to reach the goal.

Action Set Split: The whole action set is randomly divided into a 2:1:1 split of train, validation, and test action sets.

Action Observations: The observations about each action demonstrate an agent performing the 5-step skill in an 80x80 grid with no obstacles. Each observation is a trajectory of states resulting from the skill being applied, starting from a random initial state on the grid. A set of 1024 such trajectories characterizes a single skill. By observing

the effects caused on the environment through a skill, the action representation module can extract the underlying skill behavior, which is further used in the actual navigation task. Different types of action representations are described and visualized in Section B.

A.2. Recommender System

We adapt the Recommender System environment from [Rohde et al. \(2018\)](#) that simulates users responding to product recommendations (the schematic shown in Figure 12). Every episode, the agent makes a series of recommendations for a new user to maximize their cumulative click-through rate. Within an episode, there are two types of states a user can transition between: organic session and bandit session. In the bandit session, the agent recommends one of the available products to the user, which the user may select. After this, the user can transition to an organic session, where the user independently browses products. The agent takes action (product recommendation) whenever the user transitions to the bandit session. Every user interaction with organic or bandit sessions varies their preferences slightly, resulting in a change to the user’s vector. As a result, the agent cannot repetitively recommend the same products in an episode, since the user is unlikely to click it again. The environment provides engineered action representations, which are also used by the environment to determine the likelihood of a user clicking on the recommendation. The episode terminates after 100 recommendations or stochastically in between the session transitions.

State: The state is a 16-dimensional vector representing the user, \mathbf{v}_{user} . Every episode, a new user is created with a vector $\mathbf{v}_{user} \sim \mathcal{N}(\mathbf{0}, \mathbf{I})$. After each step in the episode, the user transitions between organic and bandit sessions, where the user vector is perturbed by resampling $\mathbf{v}_{user} \sim \mathcal{N}(\mathbf{v}_{user}, \sigma_1 \sigma_2 \mathbf{I})$, where $\sigma_1 = 0.1$ and $\sigma_2 \sim \mathcal{N}(0, 1)$.

Actions: There are a total of 10,000 actions (products) to recommend to users. Each action is associated with a 16 dimension representation, $c \sim \mathcal{N}(\mathbf{0}, \mathbf{I})$. The selected product’s representation and the current user vector determine the probability of a click. The agent’s objective is to recommend articles that maximize the user’s click-through rate. The probability of clicking a recommended product i with action representation c_i is given by:

$$p_{click}(\mathbf{v}_{user}, \mathbf{c}_i) = f(\mathbf{c}_i \cdot \mathbf{v}_{user} + \mu_i), \text{ where} \quad (6) \\ f(x) = \sigma(a * \sigma(b * \sigma(c * x) - d) - e),$$

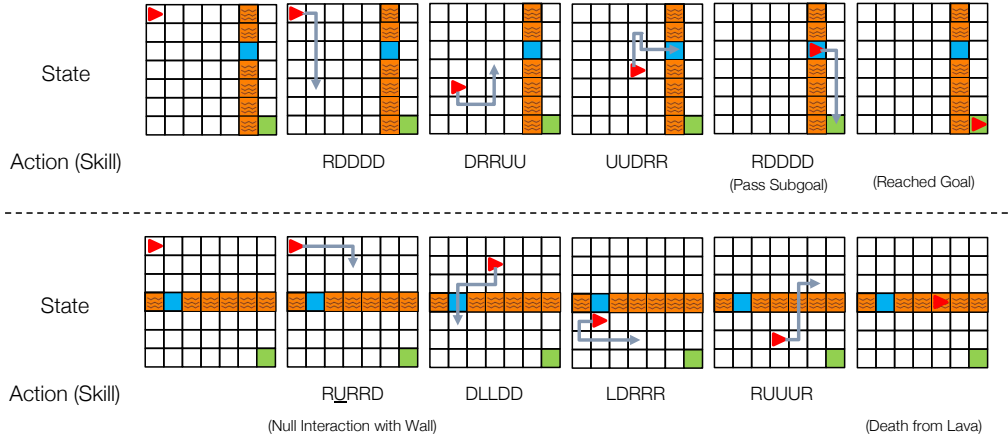


Figure 11. Grid World Environment: 9x9 grid navigation task. The agent is the red triangle, and the goal is the green cell. The environment contains one row or column of lava wall with a single opening acting as a subgoal (blue). Each action consists of a sequence of 5 consecutive moves in one of the four directions: U(p), D(own), R(ight), L(eft).

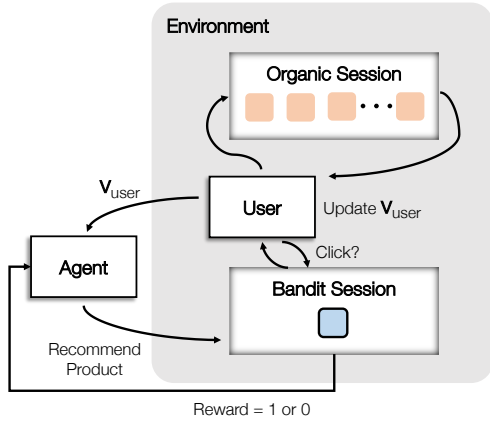


Figure 12. Recommender System schematic: The user transitions stochastically between two sessions: organic and bandit. Each transition updates the user vector. Organic sessions simulate the user independently browsing other products. Bandit sessions simulate the agent recommending products to the current user. A reward is given if the user clicks on the recommended product.

where $a = 14, b = 2, c = 0.3, d = 2, e = 6, \sigma$ is the sigmoid function, \cdot denotes a vector dot product. Here, μ_i is an action-specific constant kept hidden from the agent to simulate partial observability, as would be the case in real-world recommender systems. Constants used in the function f make the click-through rate, p_{click_s} , to be a reasonable number, adapted and modified from Rohde et al. (2018).

In Section C.5, we also provide results on the fully observable recommender system environment, where the agent has access to μ_i as well. Concretely, μ_i is concatenated to c_i to form the action representation which the learning agent utilizes to generalize.

Reward: There is a dense reward of 1 on every recommendation that receives a user click, which is determined by p_{click} computed in Eq 6.

Action Set Split: The 10,000 products are randomly divided into a 2:1:1 split of train, validation, and test action sets.

A.3. Chain REAction Tool Environment (CREATE)

Inspired by the popular video game, *The Incredible Machine*, Chain REAction Tool Environment (CREATE) is a physics-based puzzle where the objective is to get a target ball (red) to a goal position (green), as depicted in Figure 13. Some objects start suspended in the air, resulting in a falling movement when the game starts. The agent is required to select and place tools to redirect the target ball towards the goal, often using other objects in the puzzle (like the blue ball in Figure 13). The agent acts every 40 physics simulation steps to make the task reasonably challenging and uncluttered. An episode is terminated when the agent accomplishes the goal, or after 30 actions, or when there are no moving objects in the scene, ending the game. CREATE was created with the Pymunk 2D physics library (Blomqvist) and Pygame physics engine (Shinners).

CREATE environment features 12 tasks, as shown in Figure 17. Results for 3 main tasks are shown in Figure 4, 6 and 9 others in Figure 18. Concurrently developed related environments (Allen et al., 2019; Bakhtin et al., 2019) focus on single-step physical reasoning with a few simple polygon tools. In contrast, CREATE supports multi-step RL, features many diverse tools, and requires continuous tool placement.

State: At each time step, the agent receives an 84x84x3 pixel-based observation of the game screen. Here, each originally colored observation is turned into gray-scale and the

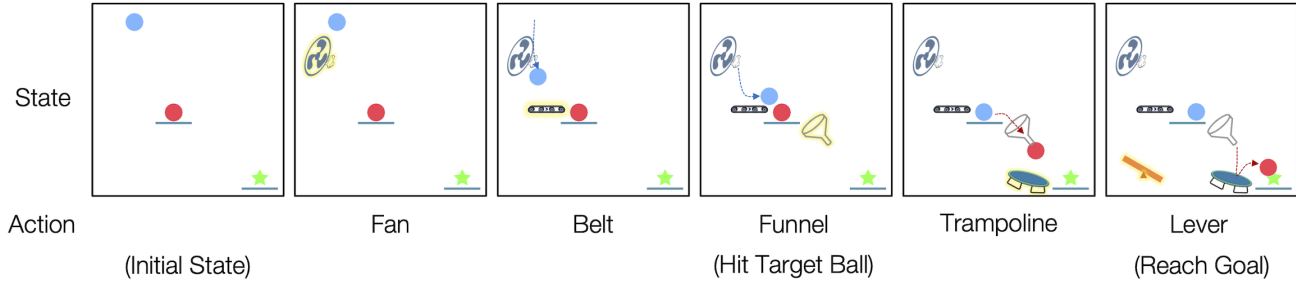


Figure 13. CREATE Push Environment: The blue ball falls into the scene and is directed towards the target ball (red), which is pushed towards the goal location (green star). This is achieved with the use of various physical tools that manipulate the path of moving objects in peculiar ways. At every step, the agent decides which tool to place and the (x, y) position of the tool on the screen.

past 3 frames are stacked channel-wise to preserve velocity and acceleration information in the state.

Actions: In total, CREATE consists of 2,111 distinct tools (actions) belonging to the classes of: ramp, trampoline, lever, see-saw, ball, conveyor belt, funnel, 3-, 4-, 5-, and 6-sided polygon, cannon, fan, and bucket. 2,111 tools are obtained by generating tools of each class with appropriate variations in parameters such as angle, size, friction, or elasticity. The parameters of variation are carefully chosen to ensure that any resulting tool is significantly different from other tools. For instance, no two tools are within 15° difference of each other. There is also a *No-Operation* action, resulting in no tool placement.

The agent outputs in a hybrid action space consisting of (1) the discrete tool selection from the available tools, and (2) (x, y) coordinates for placing the tool on the game screen.

Reward: CREATE is a sparse reward environment where rewards are given for reaching the goal, reaching any sub-goal once, and making the target ball move in certain tasks. Furthermore, a small reward is given to continue the episode. There is a penalty for trying to overlap a new tool over existing objects in the scene and an invalid penalty for placing outside the scene. The agent receives the following reward:

$$R(s, a) = \lambda_{alive} + \lambda_{Goal} \cdot \mathbf{1}_{Goal} \cdot \lambda_{Subgoal} \cdot \mathbf{1}_{Subgoal} \cdot \lambda_{target\ hit} \cdot \mathbf{1}_{target\ hit} + \lambda_{invalid} \cdot \mathbf{1}_{invalid} + \lambda_{overlap} \cdot \mathbf{1}_{overlap} \quad (7)$$

where $\lambda_{alive} = 0.01$, $\lambda_{Goal} = 10.0$, $\lambda_{Subgoal} = 2.0$, $\lambda_{target\ hit} = 1$, and $\lambda_{invalid} = \lambda_{overlap} = -0.01$.

Action Set Split: The tools are divided into a 2:1:1 split of train, validation, and test action sets. In *Default Split* presented in the main experiments, the tools are split such that the primary parameter (angle for most) is randomly split between training and testing. This ensures that the test tools are considerably different from the training tools in the same class. The validation set is obtained by randomly

splitting the testing set into half. In *Full Split*, 1,739 of the total tools are divided into a 2:1:1 split by tool class, as described in Table 1.

Train	Ramp, Trampoline, Ball, Bouncy Ball, See-saw, Cannon, Bucket
Validation and Test	Triangle, Bouncy Triangle, Lever, Fan, Conveyor Belt, Funnel

Table 1. Tool classes in the CREATE Full split.

Additionally, we used a total of 7566 tools generated at 3° angle differences for analysis experiments to study generalization properties. HVAE was trained as an oracle encoder over the entire action set, to get action representations suitable for all three analyses. The policy’s performance was studied independently by training it on 762 distinct tools with at least 15° angle differences and evaluated based on analysis-specific action sampling from the rest of the tools (e.g. at least 5° apart).

Action Observations: Each tool’s observations are obtained by testing its functionality through scripted interactions with a probe ball. The probe ball is launched at the tool from various angles, positions, and speeds. The tool interacts with the ball and changes its trajectory depending on its properties, e.g. a cannon will catch and re-launch the ball in a fixed direction. Thus, these deflections of the ball can be used to infer the characteristics of the tool. Examples of these action observations are shown at <https://sites.google.com/view/action-generalization/create>.

The collected action observations have 1024 ball trajectories of length 7 for each tool. The trajectory is composed of the environment states, which can take the form of either the 2D ball position (default) or 48x48 gray-scale images. The action representation module learns to reconstruct the corresponding data mode, either state trajectories or videos, for obtaining the corresponding action representations. Dif-

ferent types of action representations used are described and visualized in Section B.

A.4. Shape Stacking

In Shape Stacking, the agent must place shapes to build a tower as high as possible. The scene starts with two cylinders of random heights and colors, dropped at random locations on a line, which the agent can utilize to stack towers. For each action, the agent selects a shape to place and where to place it. The agent acts every 300 physics simulator steps to give time for placed objects to settle into a stable position. The episode terminates after 10 shape placements.

State: The observation at each time step is an 84x84 grayscale image of the shapes lying on the ground. We stack past 4 frames to preserve previous observations in the state.

Actions: The action consists of a discrete selection of the shape to place, the x position on the horizontal axis to drop the shape, and a binary episode termination action. The height of the drop is automatically calculated over the topmost shape, enabling a soft drop. If a shape has already been placed, trying to place it again does nothing. There are a total of 810 shapes of classes: triangle, tetrahedron, rectangle, cone, cylinder, dome, arch, cube, sphere, and capsule. These shapes are generated by varying the scale and vertical orientation in each shape class. The parameter variance is carefully chosen to ensure all the shapes are sufficiently different from each other.

In Figure 23, we compare various hybrid action spaces with shape selection. We study different ways of placing a shape: dropping at a fixed location, or deciding x -position, or deciding (x, y) -positions.

Reward: To encourage stable and tall towers, there is a sparse reward at episode end, for the final height of the topmost shape in the scene, added to the average heights of all N shapes in the scene:

$$R(s) = (\lambda_{top} \max(h_i) + \lambda_{avg} \frac{1}{N} \sum_i h_i) \cdot \mathbf{1}_{Done}, \quad (8)$$

where h_i is the height of shape i and $\lambda_{top} = \lambda_{avg} = 0.5$.

Action Set Split: The shapes are divided into a 2:1:1 split of train, validation, and test action sets. In Default Split presented in the main experiments, the shapes are split such that the primary parameter of scale is randomly split between training and testing. This ensures that test tools are considerably different in scale from the train tools in the same class. The validation set is obtained by randomly splitting the test set into half. In Full Split, the split is determined by shape class, as shown in Table 2.

Train	Domes, Rectangles, Capsules, Triangles, Arches, Spheres
Validation and Test	Cylinders, Tetrahedrons, Cubes, Cones, Angled-Rectangles, Angled-Triangles

Table 2. Shape classes in the Shape Stacking Full split.

Action Observations: In Shape Stacking the functionality of each action is characterized by the physical appearance of the shape. Thus, the action observations consist of images of the shape from various camera angles and heights. Each shape has 1,024 observed images of resolution 84x84. Examples of these action observations are shown at <https://sites.google.com/view/action-generalization/shape-stacking>.

B. Visualizing Action Representations

In this work, we train and evaluate a wide variety of action representations based on environments, data-modality, presence or absence of hierarchy in action encoder, and different action splits. We describe these in detail and provide t-SNE visualizations of the inferred action representations of previously unseen actions. These visualizations show how our model can extract information about properties of the actions, by clustering similar actions together in the latent space. Unless mentioned otherwise, the HVAE model is used to produce these representations.

Grid World: Figure 14 shows the inferred action or skill representations in Grid World. The actions are colored by the relative change in the location of the agent after applying the skill. For example, the skill "Up, Up, Up, Right, Down" would translate the agent to the upper right quadrant from the origin, hence visualized in red color. All learned action representations are 16-dimensional. We plot the following action representations:

- State Trajectories (default): HVAE encodes action observations consisting of trajectories of 2D (x, y) coordinates of the agent on the 80x80 grid.
- Non-Hierarchical VAE (baseline): A standard VAE encodes all the state-based action observations individually, and then computes the action representation by taking their mean.
- One-hot (alternate): State is represented by two 80-dimensional one-hot vectors of the agent's x and y coordinates on the 80x80 grid. Reconstruction is based on a softmax cross-entropy loss over the one-hot observations in the trajectory.
- Engineered (alternate): These are 5-dimensional representations containing the ground-truth knowledge of the five moves (up, down, left, right) that constitute a skill. The clustering of our learned representations looks comparable to these oracle representations.

Generalization to New Actions in Reinforcement Learning

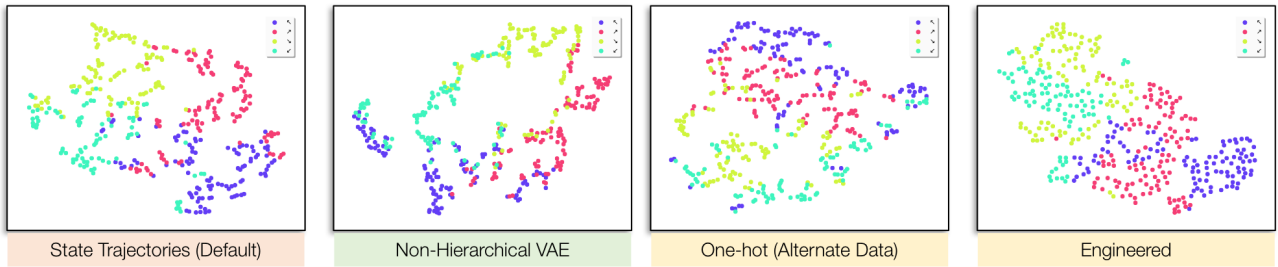


Figure 14. t-SNE Visualization of learned skill representation space for Grid World environment. Colored by the quadrant that the skill translates the agent to.

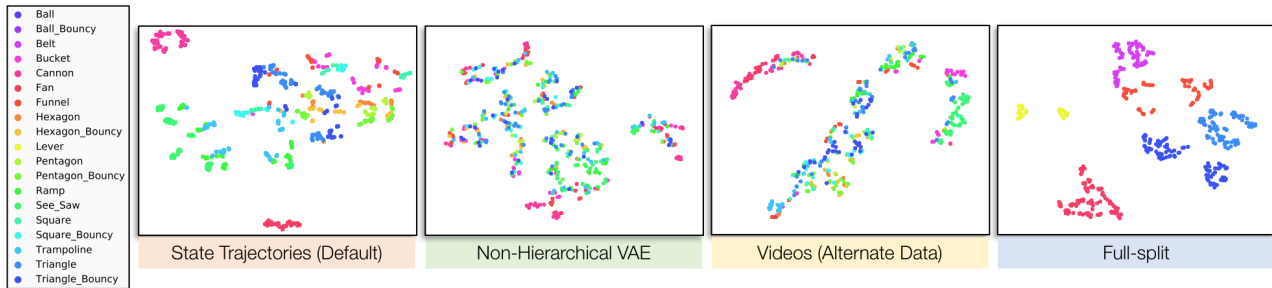


Figure 15. t-SNE Visualization of learned tool representation space for CREATE environment. Colored by the tool class.

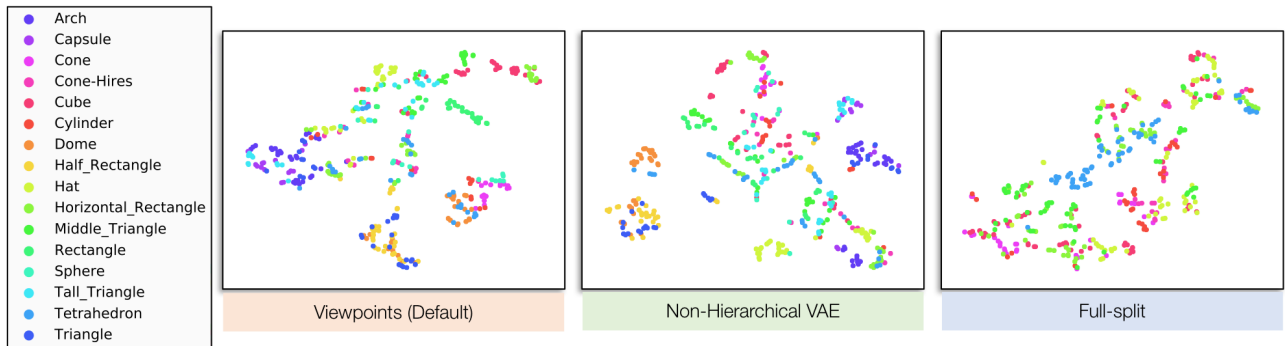


Figure 16. t-SNE Visualization of learned action representation space for the Shape-stacking environment. Colored by the shape class.

CREATE: Figure 15 shows the inferred action or tool representations in CREATE. The actions are colored by tool class. All action representations are 128-dimensional.

- State Trajectories (default): HVAE encodes action observation data composed of (x, y) coordinate states of the probe ball's trajectory.
- Non-Hierarchical VAE (baseline): A standard VAE encodes all the state-based action observations individually, and then computes the action representation by taking their mean.
- Video (alternate): HVAE encodes action observation data composed of 84x84 grayscale image-based trajec-

tories (videos) of the probe ball interacting with the tool. The data is collected identically as the state case, only the modality changes from state to image frames.

- Full Split: HVAE encodes state-based action observations, however, the training and testing tools are from the *Full Split* experiment. The visualizations show that even though training tools are vastly different from evaluation tools, HVAE generalizes and clusters well on unseen tools.

Shape Stacking: Figure 16 shows the inferred action representations in Shape Stacking. The shapes are colored according to shape class. All action representations are 128-dimensional.

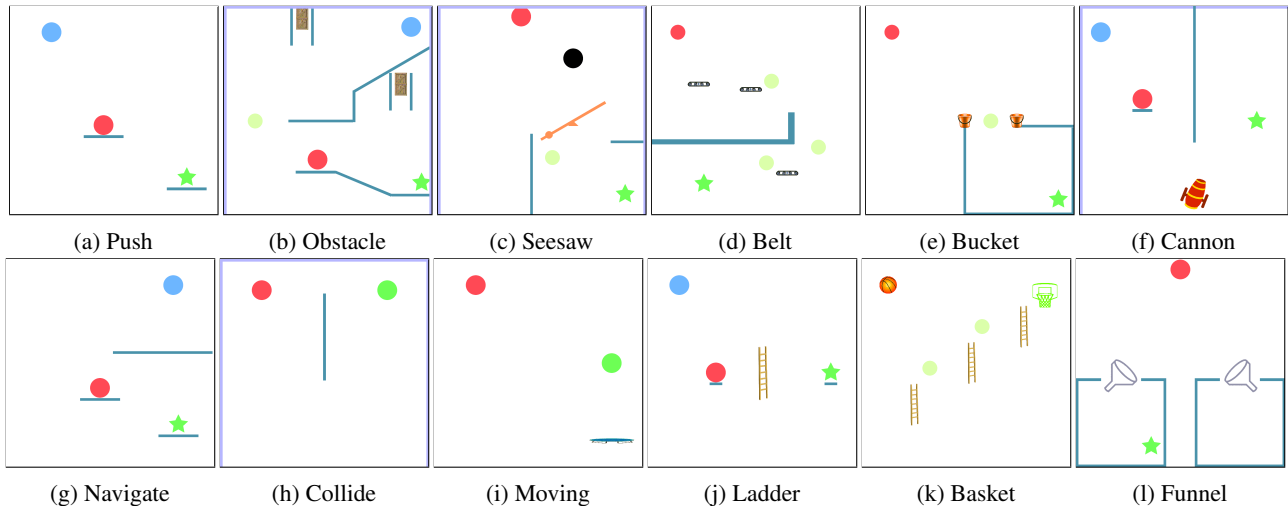


Figure 17. 12 CREATE tasks. Complete results on (a) - (c) are in Figure 4, 6, while (d) - (l) are in Figure 18.

- Viewpoints (default): HVAE encodes action observations in the form of viewpoints of the shape from different camera angles and positions.
- Non-Hierarchical VAE (baseline): A standard VAE encodes all the image-based action observations individually, and then computes the action representation by taking their mean.
- Full-split: The training and testing tools are from the *Full Split* experiment. Previously unseen shape types are clustered well, showing the robustness of HVAE.

C. Further Experimental Results

C.1. Additional CREATE Results

Figure 17 visually describes all the CREATE tasks. The objective is to make the target ball (red) reach the goal (green), which may be fixed or mobile. Figure 18 demonstrates our method’s results on the remaining nine CREATE tasks (the initial three tasks are in Figure 4, 6). Strong training and testing performance on a majority of these tasks shows the robustness of our method. The developed CREATE environment can be easily modified to generate more such tasks of varying difficulties. Due to the diverse set of tools and tasks, we propose CREATE and our results as a useful benchmark for evaluating action space generalization in reinforcement learning.

C.2. Additional Finetuning Results

We present additional results of finetuning and training from scratch to adapt to unseen actions across all CREATE Obstacle, CREATE Seesaw, Shape Stacking, Grid World, and Recommender. In the results presented in Figure 19, we observe the same trend holds where additional training takes

many steps to achieve the performance our method obtains zero-shot.

C.3. CREATE: No Subgoal Reward

To verify our method’s robustness, we also run experiments on a version of the CREATE environment without the subgoal rewards. The results in Figure 20 verify that even without reward engineering, our method exhibits strong generalization, albeit with higher variance in train and testing performance.

C.4. Auxiliary Policy Alternative Architecture

While in our framework, the auxiliary policy is computed from the state encoding alone, here we compare to also taking the selected discrete-action as input to the auxiliary policy. Comparison of this alternative auxiliary policy to the auxiliary policy from the main paper is shown in Figure 21. There are minimal differences in the average success rates of the two design choices.

C.5. Fully Observable Recommender System

Figure 22 demonstrates our method in a fully observable recommender environment where the product constant μ_i from Eq. 6 is also included in the engineered action representation. All methods achieve better training and generalization performance compared to the original partially observable Recommender System environment. However, full observability is infeasible in practical recommender systems. Therefore, we focus on the partially observed environment in the main results.

Generalization to New Actions in Reinforcement Learning

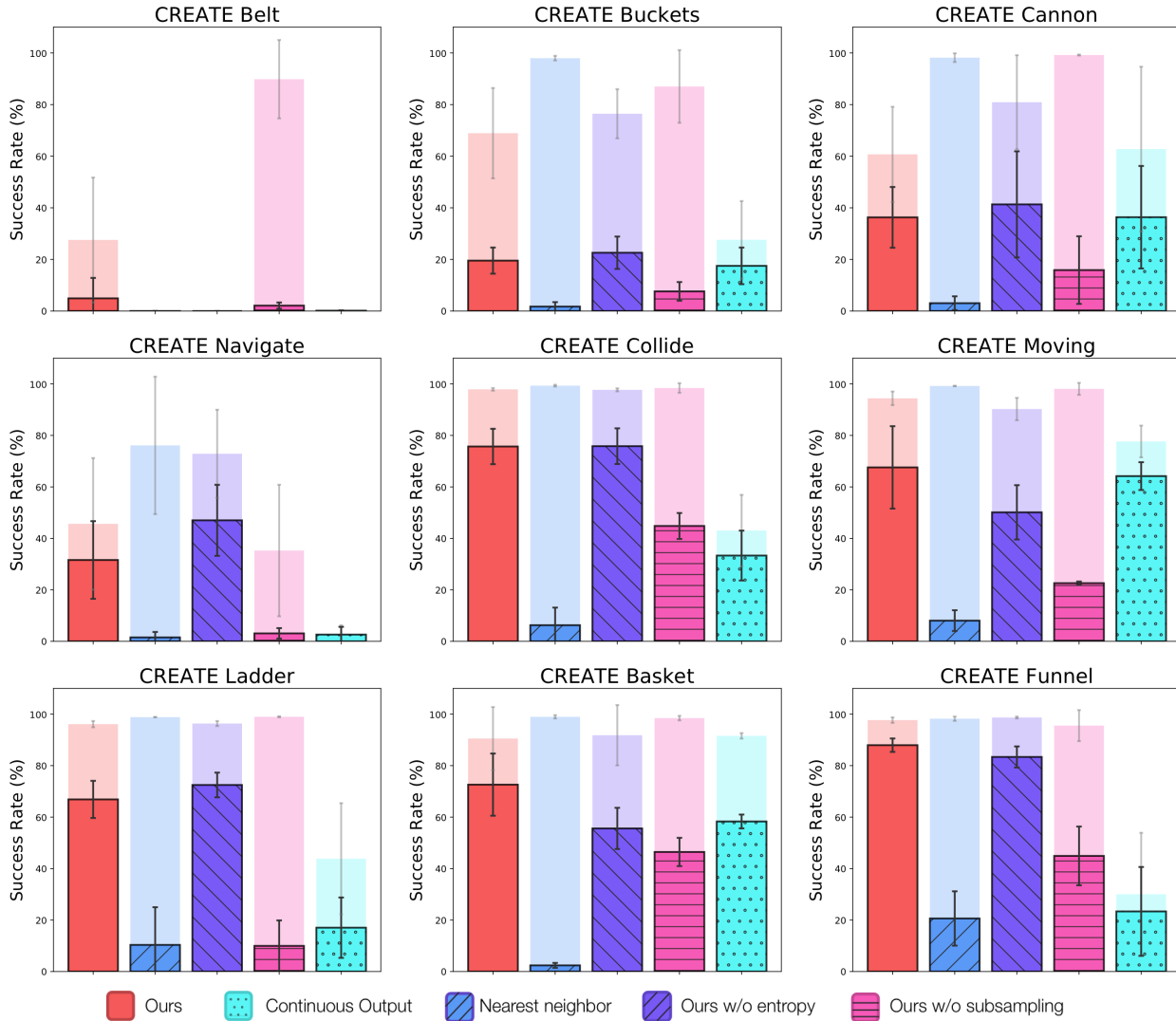


Figure 18. Results on the remaining 9 CREATE tasks with the same evaluation details as the main paper (Figure 4). We compare our method against all the baselines (Section 5.3) and ablations (Section 5.4).

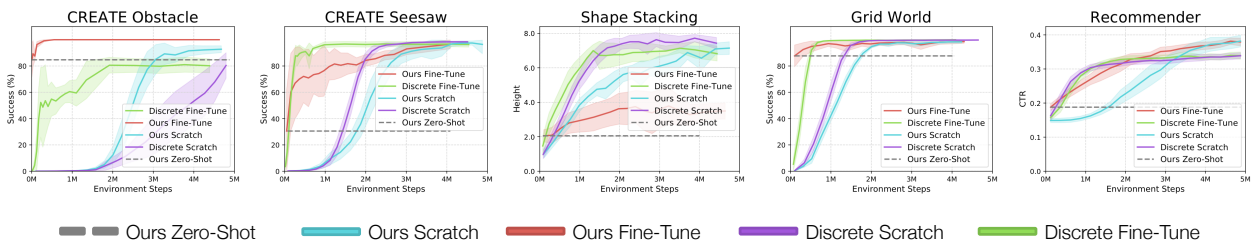


Figure 19. Finetuning or training the policy from scratch on the new action space across the remaining 5 tasks (Figure 10 only shows results on CREATE Push). The evaluation settings are the same as described in Section 6.4.

C.6. Additional Shape Stacking Results

Figure 23 demonstrates performance on different shape placement strategies in Shape Stacking using our frame-

work. In *No Place*, the shapes are dropped at the center of the table, and the agent only selects which shape to drop from the available set. Since there are two randomly placed cylinders on the table, this setting of drop-

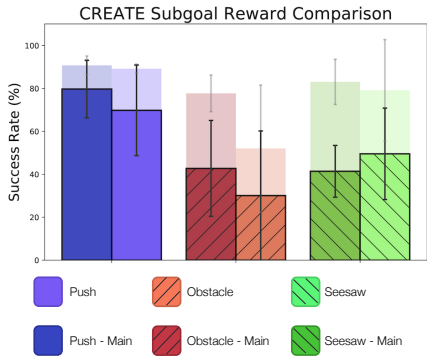


Figure 20. Comparison of a version of CREATE that does not use subgoal rewards. The “Main” methods are from the main paper using subgoal rewards (Figure 4).

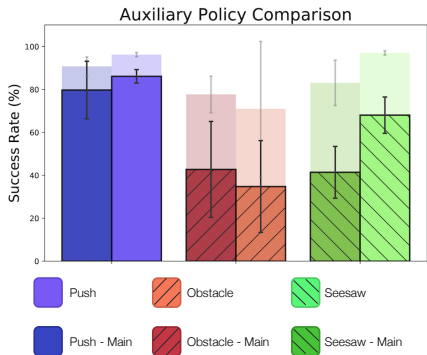


Figure 21. Comparison of an alternative auxiliary network architecture that is conditioned on the selected discrete action. The “Main” results are the default results that do not condition the auxiliary policy on the selected action (Figure 4).

ping in the center gives less control to the agent while stacking tall towers. Thus we report default results on *1D Place*, where the agent outputs in a hybrid action space consisting of shape selection and 1D placement through x -coordinate of the dropping location. The y -coordinate of the drop is fixed to the center. Finally, in *2D Place*, the agent decides both x and y coordinates to have more control but makes the task more challenging due to the larger search space. The evaluation videos of these new settings are available on <https://sites.google.com/view/action-generalization/shape-stacking>.

Figure 23 also shows the results of our method trained and evaluated on *Full Split* which was introduced in Table 2. Poor performance on this split could be explained by the policy not seeing enough shape classes during training to be able to generalize well to new shape classes during testing. This is also expected since this split severely breaks the i.i.d. assumption essential for generalization (Bousquet et al., 2003).

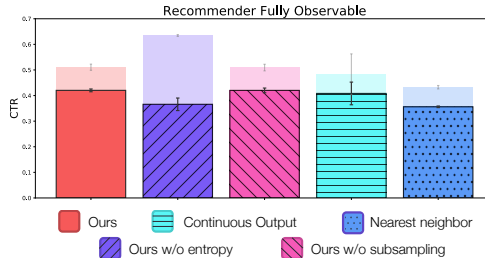


Figure 22. Training and testing results on the fully observable version of Recommender System with standard evaluation settings.

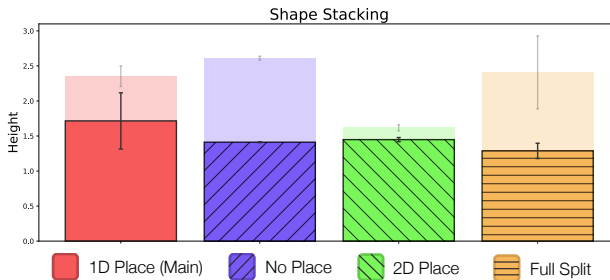


Figure 23. Comparing different placement strategies in shape stacking and showing performance on the *Full Split* action split. Results are using our method with the standard evaluation details.

C.7. Learning Curves

Figure 24 show the training and validation performance curves for all methods and environments to contrast the training process of a policy against the objective of generalization to new actions. The plots clearly show how the generalization gap varies over the training of the policy. Ablation curves (last two columns) for some environments depict that an increase in training performance corresponds to a drop in validation performance. This is attributed to the policy overfitting to the training set of actions, which is often observed in supervised learning. Our proposed regularizing training procedure aims to avoid such overfitting.

D. Experiment Details

D.1. Implementation

We use PyTorch (Paszke et al., 2017) for our implementation, and the experiments were primarily conducted on workstations with 72-core Intel Xeon Gold 6154 CPU and 4 NVIDIA GeForce RTX 2080 Ti GPUs. Each experiment seed takes about 6 hours (Recommender) to 25 hours (CREATE) to converge. For logging and tracking experiments, we use the Weights & Biases tool (Biewald, 2020). All the environments were developed using the OpenAI Gym interface (Brockman et al., 2016). The HVAE implementation is based on the PyTorch implementation of Neural

Generalization to New Actions in Reinforcement Learning

Hyperparameter	Grid world	Recommender	CREATE	Shape Stacking
HVAE				
action representation size	16	16	128	128
batch size	128	-	128	32
epochs	10000	-	10000	5000
Policy				
entropy coefficient	0.05	0.01	0.005	0.01
observation space	81	16	$84 \times 84 \times 3$	$84 \times 84 \times 4$
actions per episode	50	500	50	20
total environment steps	4×10^7	4×10^7	6×10^7	3×10^6
max. episode length	10	100	30	10
continuous entropy scaling	-	-	0.1	0.1
PPO batch size	4096	2048	3072	1024

Table 3. Environment-specific hyperparameters

Statistician (Edwards & Storkey, 2017), and we use RAdam optimizer (Liu et al., 2019). For training the policy network, we use PPO (Schulman et al., 2017; Kostrikov, 2018) with the Adam optimizer (Kingma & Ba, 2015). Further details can be found in the supplementary code.⁴

D.2. Hyperparameters

The default hyperparameters shared across all environments are shown in Table 4 and environment-specific hyperparameters are given in Table 3. We perform linear decay of the learning rate over policy training.

Hyperparameter	Value
HVAE	
learning rate	0.001
action observations	1024
MLP hidden layers	3
q_ϕ hidden layer size	128
default hidden layer size	64
Policy	
learning rate	0.001
discount factor	0.99
parallel processes	32
hidden layer size	64
value loss coefficient	0.5
PPO epochs	4
PPO clip parameter	0.1

Table 4. General Hyperparameters

⁴Code available at <https://github.com/clvrain/new-actions-rl>

D.2.1. HYPERPARAMETER SEARCH

Initial HVAE hyperparameters were inherited from the implementation of Edwards & Storkey (2017) and PPO hyperparameters from Kostrikov (2018). The hyperparameters were finetuned to optimize the performance on the held-out validation set of actions. Certain hyperparameters were sensitive to the environment or the method being trained and were searched for more carefully.

Specifically, entropy coefficient is a sensitive parameter to appropriately balance the ease of reward maximization during training versus the generalizability at evaluation. For each method and environment, we searched for entropy coefficients in subsets of $\{0.0001, 0.001, 0.005, 0.01, 0.05, 0.1\}$, and selected the best parameter based on the performance on the validation set. We found PPO batch size to be an important parameter affecting the speed of convergence, convergence value, and variance across seeds. Thus, we searched for the best value in $\{1024, 2048, 3072, 4096\}$ for each environment. Total environment steps are chosen so all the methods and baselines can run until convergence.

D.3. Network Architectures

D.3.1. HIERARCHICAL VAE

Convolutional Encoder: When the action observation data is in image or video form, a convolution encoder is applied to encode it into a latent state or state-trajectory. Specifically, for CREATE video case, each action observation is a 48x48 grayscale video. Thus, each frame of the video is encoded through a 7-layer convolutional encoder with batch norm (Ioffe & Szegedy, 2015). Similarly, for Shape Stacking, the action observation is an 84x84 image, that is encoded through 9 convolutional layers with batch norm.

Bi-LSTM Encoder: When the data is in trajectory form (as in CREATE and Grid World), the sequence of states are encoded through a 2-layer Bi-LSTM encoder. For CREATE video case, the encoded image frames of the video are passed through this Bi-LSTM encoder in place of the raw state vector. After this step, each action observation is in the form of a 64-dimensional encoded vector.

Action Inference Network: The encoded action observations are passed through a 4-layer MLP with ReLU activation, and then aggregated with mean-pooling. This pooled vector is passed through a 3-layer MLP with ReLU activation, and then 1D batch-norm is applied. This outputs the mean and log-variance of a Gaussian distribution q_ϕ , which represents the entire action observation set, and thus the action. This is then used to sample an action latent to condition reconstruction of individual observations.

Observation Inference Network: The action latent and individual encoded observations are both passed through linear layers and then summed up, and followed by a ReLU nonlinearity. This combined vector is then passed through two 2-layer MLPs with ReLU followed by a linear layer, to output the mean and log-variance of a Gaussian distribution, representing the individual observation conditioned on the action latent. This is used to sample an observation latent, which is later decoded back while being conditioned on the action latent.

Observation Decoder: The sampled observation latent and its action latent are passed through linear layers, summed and then followed by a nonlinearity. For non-trajectory data (as in Shape Stacking), this vector is then passed through a 3-layer MLP with ReLU activation to output the decoded observation’s mean and log-variance (i.e. a Gaussian distribution). For trajectory data (as in CREATE and Grid World), the initial ground truth state of the trajectory is first encoded with a 3-layer MLP with ReLU. Then an element-wise product is taken with the action-observation combined vector. The resulting vector is then passed through an LSTM network to produce the latents of future states of the trajectory. Each future state latent of the trajectory goes through a 3-layer MLP with ReLU, to result in the mean and log-variance of the decoded trajectory observation (i.e. a Gaussian distribution).

Convolutional Decoder: If the observation was originally an image or video, then the mean of the reconstructed observation is converted into pixels through a convolutional decoder consisting of 2D convolutional and transposed-convolutional layers. For the case of video input, the output of the convolutional decoder is also channel-wise augmented with with a 2D pixel mask. This mask is multiplied with the mean component of the image output (i.e. log-variance output stays the same), and then added to the initial frame of the video. This is the temporal skip connection tech-

nique (Ebert et al., 2017), which eases the learning process with high-dimensional video observation datasets.

Finally, the reconstruction loss is computed using the Gaussian log-likelihood of the input observation data with respect to the decoded distribution.

D.3.2. POLICY NETWORK

State Encoder f_ω : When the input state is in image-form (channel-wise stacked frames in CREATE and Stacking), f_ω is implemented with a 5-layer convolutional network, followed by a linear layer and ReLU activation function. When the input is not an image, we use 2-layer MLP with tanh activation to encode the state.

Critic Network V : For image-based states, the output of the state encoder f_ω is passed through a linear layer to result in the value function of the state. This is done to share the convolutional layers between the actor and critic. For non-image states, we use 2-layer MLP with tanh activation, followed by a linear layer to get the state’s value.

Utility Function f_ν : Each available action’s representation c is passed through a linear layer and then concatenated with the output of the state encoder. This vector is fed into a 2-layer MLP with ReLU activation to output a single logit for each action. The logits of all the available actions are then stacked and input to a Categorical distribution. This acts as the policy’s output and is used to sample actions, compute log probabilities, and entropy values.

Auxiliary Policy f_χ : The output of the state encoder is also separately used to compute auxiliary action outputs. For CREATE and Shape Stacking, we have a 2D position action in $[-1, 1]$. For such constrained action space, we use a Beta distribution whose α and β are computed using linear layers over the state encoding. Concretely, $\alpha = 1 + \text{softplus}(\text{fc}_\alpha(f_\omega(s)))$ and $\beta = 1 + \text{softplus}(\text{fc}_\beta(f_\omega(s)))$, to ensure their values lie in $[1, \infty]$. This in turn ensures that the Beta distribution is unimodal with values constrained in $[0, 1]$ (as done in (Chou et al., 2017)), which we then convert to $[-1, 1]$. The Shape Stacking environment also has a binary termination action for the agent. This is implemented by passing the state encoding through a linear layer which outputs two logits (for continuation/termination) of a Categorical distribution. The auxiliary action distributions are combined with the main discrete action Categorical distribution from f_ν . This overall distribution is used to sample hybrid actions, compute log probabilities, and entropy values. Note, the entropy value of the Beta distribution is multiplied by a scaling factor of 0.1, for better convergence.

Generalization to New Actions in Reinforcement Learning

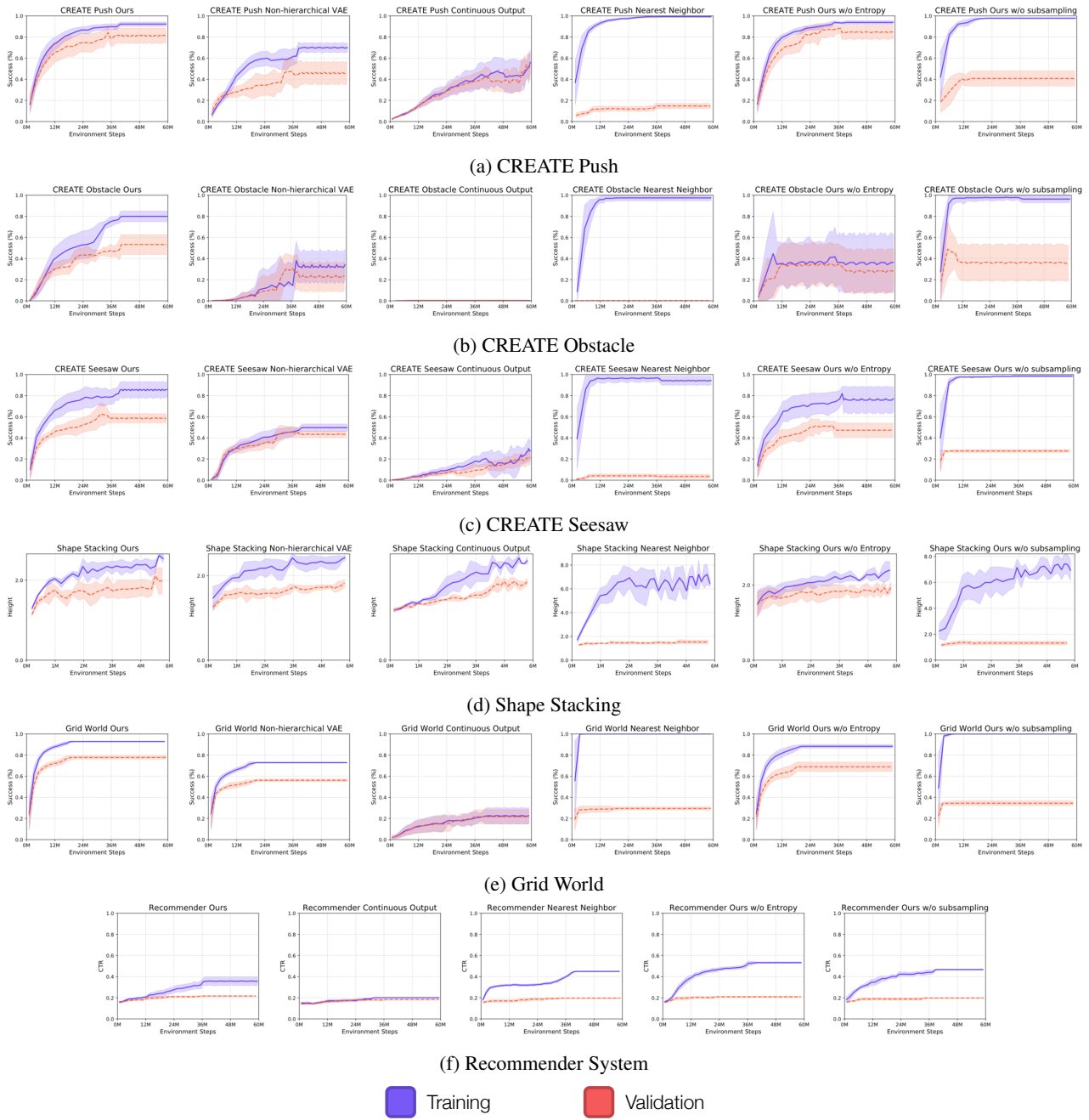


Figure 24. Learning curves for all environments and methods showing performance on both the training and validation sets. Each line shows the performance of 5 random seeds (8 for Grid World) as average value and the shaded region as the standard deviation.